Chemical Engineering Journal 328 (2017) 304–319

Contents lists available at ScienceDirect

Chemical Engineering Journal

journal homepage: www.elsevier.com/locate/cej

Increasing the carbon capture efficiency of the Ca/Cu looping process for power production with advanced process schemes

M. Martini [a], I. Martínez [b], M.C. Romano [b], P. Chiesa [b], F. Gallucci [a,*], M. van Sint Annaland [a]

[a] Chemical Process Intensification, Chemical Engineering and Chemistry, Eindhoven University of Technology, Eindhoven, The Netherlands
[b] Politecnico di Milano, Department of Energy, Milano, Italy

HIGHLIGHTS

- A 1D model is used for calculating the different stages of the Ca-Cu process.
- High T plateau during the SER stage limits the overall carbon capture efficiency.
- An alternative scheme for the Ca-Cu process is proposed for overcoming this limit.
- An overall carbon capture efficiency of 88% is obtained for this alternative scheme.

ARTICLE INFO

Article history:
Received 3 February 2017
Received in revised form 23 June 2017
Accepted 7 July 2017
Available online 8 July 2017

Keywords:
Hydrogen
Sorption enhanced reforming
Chemical looping
CO_2 capture
Modelling

ABSTRACT

The Ca-Cu process is a novel concept for hydrogen production with inherent CO_2 capture that has received great attention in the last years as potential low-CO_2 emission technology for power generation and hydrogen production from natural gas. The process is based on the reforming of natural gas in the presence of a CaO-based sorbent and a Cu/CuO chemical looping combustion loop that provides the energy needed for $CaCO_3$ calcination. The process is proposed to be carried out in adiabatic, dynamically operated fixed bed reactors operating in parallel. Simulations with a 1D dynamic pseudo-homogeneous reactor model were performed for the different stages of the Ca-Cu process, considering a reasonable set of process assumptions. It has been demonstrated that the formation of a high temperature plateau during the sorption-enhanced reforming stage of the process, caused by the decoupling between the steam methane reforming and the carbonation reactions in different positions along the bed, decreases the carbon capture efficiency that can be achieved in this process. Concretely, a maximum overall carbon capture efficiency of almost 82% could be obtained with selected operating conditions in the Ca-Cu process. With the aim of overcoming this limited capture efficiency, a novel alternative scheme for the Ca-Cu process has been proposed, consisting in splitting the sorption enhanced reforming stage into two steps with intercooling. Simulations of this case demonstrated that an overall carbon capture efficiency of 88% can be achieved.

1. Introduction

Most of the hydrogen produced worldwide (i.e. around 65 million tons per year) is used as feedstock within the chemical and refinery industries, while showing a growing interest in the coming years as energy carrier for conversion into electricity, mechanical energy or heat [1]. Natural gas represents the principal feedstock for hydrogen production, accounting for more than 48% of the worldwide production, followed by petroleum and coal as primary energy sources. Even though the CO_2 emissions associated with large scale hydrogen production worldwide represents only 3% of the global emissions [2], the expected growth in the hydrogen demand in the coming years makes the development of large fossil fuels hydrogen production plants integrated with CO_2 capture technologies particularly interesting [3]. Moreover, despite the fact that the steam methane reforming (SMR) process of natural gas is the dominant and most economic technology for large scale H_2 production, it presents important drawbacks associated to its demanding operating conditions of high pressure and high temperature in the reforming reactor. Thus, different solutions have been proposed in the literature for overcoming the thermodynamic restrictions imposed by those demanding conditions, which will

* Corresponding author.
E-mail address: F.gallucci@tue.nl (F. Gallucci).

http://dx.doi.org/10.1016/j.cej.2017.07.048
1385-8947/

Nomenclature

c_i	concentration of gas component i, mol m^{-3}
$C_{p,g}$	gas heat capacity, J kg^{-1} K^{-1}
$C_{p,s}$	solid heat capacity, J kg^{-1} K^{-1}
d_p	particle diameter, m
D_{ax}	axial mass dispersion, m^2 s^{-1}
$\Delta_r H_j$	reaction enthalpy, J/mol
M_i	molecular weight of component i, kg mol^{-1}
n	reaction order
n_i	number of moles of specie *i*
p_i	pressure of component i, Pa
p_0	atmospheric pressure, Pa
r_j	reaction rate, mol m^{-3} s^{-1}
T	temperature, K
T_{ad}	gas equilibrium temperature reached in stage A, °C
$T_{g,in,i}$	inlet gas temperature of stage *i*, °C
$T_{max,i}$	maximum temperature reached in the bed during stage *i*, °C
$T_{s,0}$	initial bed temperature, °C
v_g	superficial gas velocity, m/s
$w_{g,i}$	gas component weight fraction
X	solid conversion
y_i	molar fraction of specie *i*

Greek letters

ε_p	particle porosity
ε_g	void fraction of the bed
λ_{eff}	effective thermal conductivity, W m^{-1} K^{-1}
λ_g	thermal conductivity of the gas, W m^{-1} K^{-1}
η	effectiveness factor
Φ	Thiele modulus
ρ_g	gas density, kg m^{-3}
ρ_s	solid density, kg m^{-3}

Acronyms

CCE	carbon capture efficiency
CCE_{SER}	carbon capture efficiency of the SER stage
CCEtot	overall carbon capture efficiency
MDEA	N-methyldiethanolamine
NG	natural gas
NGCC	natural gas combined cycle
PHM	pseudo-homogeneous model
PSA	pressure swing absorption
S/C	steam to carbon molar ratio
SER	sorption enhanced reforming
SMR	steam methane reforming
WGS	water gas shift
ZEG	zero emission gas

allow significant improvements in the efficiency of this process and so in the H_2 production costs.

Chemical looping reforming is one of the technologies proposed in literature for H_2 production and CO_2 capture. In this system the heat for the reforming reactions is supplied by the oxidation of a metal-based-solid, called oxygen carrier. The metal oxide is then reduced resulting in a cyclic system [4,5]. Another way to increase the efficiencies of the SMR is to overcome equilibrium limitations by separating the H_2 produced by the reforming reactions using H_2 selective membranes in the reforming reactor. This also allows operating the reactor at lower temperatures than those required by the conventional SMR process [6–9]. An alternative approach for enhancing the thermodynamic of the system is the sorption enhanced reforming (SER), which involves the use of a Ca-based CO_2 sorbent inside the reactor to remove the CO_2 through the carbonation reaction (Eq. (3)) simultaneously with the steam reforming (Eq. (1)) and water gas shift (Eq. (2)) reactions [10,11].

$$CH_4 + H_2O \leftrightarrow CO + 3H_2, \quad \Delta H_{298K} = +206.2 \text{ kJ/mol} \tag{1}$$

$$CO + H_2O \leftrightarrow CO_2 + H_2, \quad \Delta H_{298K} = -41.5 \text{ kJ/mol} \tag{2}$$

$$CaO + CO_2 \leftrightarrow CaCO_3, \quad \Delta H_{298K} = -178.8 \text{ kJ/mol} \tag{3}$$

In order to obtain a continuous operation, the $CaCO_3$ formed needs to be regenerated to CaO. The calcination reaction is highly endothermic and therefore a large amount of heat has to be supplied in the sorbent regenerator reactor. Different solutions for fulfilling the energy demand in the calciner have been proposed in literature. Some schemes propose to supply the energy required by burning some fuel directly inside the regenerator [12–14] or by high-temperature heat exchangers using combustion gases or a heat transfer fluid as heat source [15,16]. Other studies propose the use of a Ni/NiO-based chemical looping combustion system to supply the regeneration heat in situ in the reactor through the oxidation of the Ni material with air [17], but without including CO_2 capture.

A novel scheme for the sorption-enhanced reforming of natural gas in the presence of a CaO-based CO_2 sorbent was proposed by Abanades et al. [18]. The core of this process is coupling a second Cu/CuO chemical loop to supply the energy needed for the $CaCO_3$ calcination. A conceptual scheme of this novel process is shown in Fig. 1, which was proposed to be carried out in a series of fixed bed reactors operating in parallel at different pressures and temperatures to fully exploit its inherent advantages. The first step of the process consists of the production of a hydrogen-rich stream through the sorption-enhanced reforming (SER) feeding a mixture of natural gas and steam to the reactor. Reforming, water-gas-shift and carbonation reactions (Eqs. (1)–(3)) occur simultaneously in the reactor, which operates at elevated pressures. The following step (indicated as B in Fig. 1) consists of the oxidation of Cu to CuO by feeding pressurized diluted air to the reactor. The maximum temperature achieved during this exothermic step is kept below a reasonable limit to avoid undesired reactions or agglomeration of the Cu material present in the bed, and to minimize $CaCO_3$ decomposition before the next step. Finally, the calcination of the $CaCO_3$ formed during the SER stage of the process occurs thanks to the energy released by the reduction of CuO, which is carried out by feeding a fuel gas containing H_2, CO and CH_4. This stage of the process (referred as C in Fig. 1) is performed at low pressure with the aim of limiting the temperature needed to promote $CaCO_3$ calcination. The Ca/Cu ratio of the material present in the solid bed is chosen such that the energy released by CuO reduction reactions during stage C allows reaching the desired temperature and sustaining the $CaCO_3$ calcination reaction. The inherent characteristics of the Ca-Cu process regarding operating pressure and hydrogen purity make it suitable for both hydrogen and power production [18]. A detailed and comprehensive full process design of a large-scale hydrogen production plant based on the Ca-Cu process has been already addressed in the literature [19], based on simplified reactors models that calculate the mass and energy balances of the different process stages [20]. A low-emission power production plant based on a natural gas combined cycle (NGCC) has been also

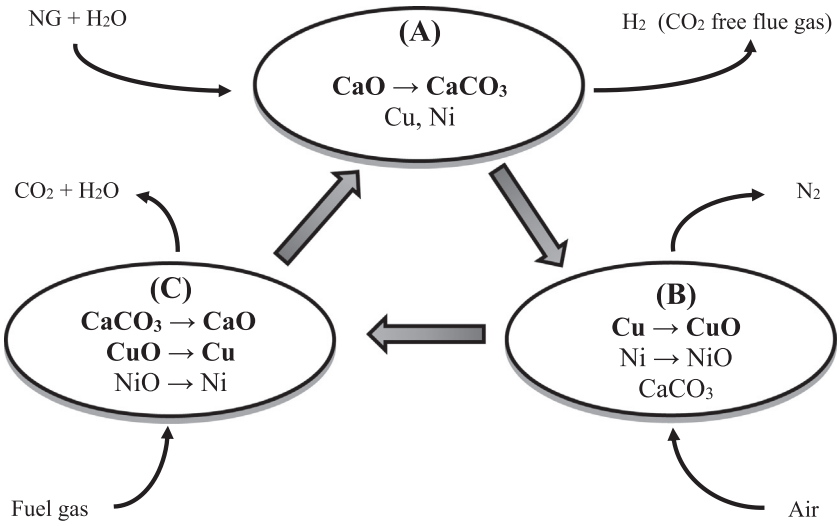

Fig. 1. Conceptual scheme of the Ca-Cu looping process.

studied with the same reactors models, integrating the Ca-Cu process as a pre-combustion CO_2 capture technology [21].

Different operating parameters and process integration strategies should be considered based on the application of the Ca-Cu process. When integrated in a hydrogen production plant, the high-pressure hydrogen obtained during the first stage of the process needs to be purified to remove impurities and unconverted CH_4 resulting from this process step. As in conventional large-scale commercial hydrogen production plants, a pressure swing adsorption (PSA) unit can be used to purify the hydrogen-rich gas obtained to a purity as high as 99.999%, adequate to be ultimately used as process gas in chemical processes or as fuel for advanced power generation technologies (e.g. low temperature fuel cells). In this configuration, the off-gas coming from the PSA unit, containing unconverted CH_4, CO, CO_2 and non-recovered H_2, can be used as fuel in the reduction stage of the Ca-Cu process, avoiding in this way CO_2 emissions resulting from the carbon slip in the SER stage [19]. Therefore, when integrated in a hydrogen plant, the achievement of high carbon capture ratio in the SER stage is not essential to obtain a high overall CO_2 capture ratio. However, when the Ca-Cu process is integrated in a power plant, the rich-H_2 gas produced in the SER stage is used as fuel in the combustion chamber of a gas turbine without any downstream purification step. In this case, the carbon compounds in the H_2-rich gas from the SER stage are ultimately emitted to the atmosphere with the gas turbine flue gas. Therefore, for application in power generation plants, reaching a high CO_2 capture rate in stage A of the Ca-Cu process is crucial to limit CO_2 emissions. In this work, the Ca-Cu process is aimed to be part of an electricity production plant, as a pre-combustion CO_2 capture process for reducing carbon emissions. In this way, all the simulations efforts have been mainly focused on the SER stage A of this process, which needs to be carefully assessed for improving its CO_2 capture efficiency and therefore the CCE of the whole process, as demonstrated further on in this paper.

Accurate simulations using a 1-D pseudo-homogeneous reactor model (PHM) have been carried out by some of the authors of this work studying the different stages of the Ca-Cu process in detail [22]. This model describes the performance of an adiabatic fixed bed reactor process, accounting for axial mass and heat dispersion and reaction kinetics for both gas and solid phases. Preliminary results obtained by this model for the Ca-Cu process have demonstrated that the overall carbon capture efficiency of the process is limited to about 80%, due to the existence of a high temperature plateau during the SER stage that restricts the maximum CO_2 separation efficiency that can be reached. This result may negatively affect its application into a power production scheme, since this rather low CO_2 capture efficiency makes the Ca-Cu process not competitive with benchmark pre-combustion CO_2 capture technologies based on amine absorption, where CO_2 capture efficiencies as high as 90% are easily achievable [23,24].

With the intent of overcoming these limits on the carbon capture efficiency, the main objective of this work is using the aforementioned 1-D PHM to study more thoroughly the performance of the SER stage of the Ca-Cu process and the carbon capture efficiency that can be achieved. A broad range of operating conditions as well as modifications to the traditional process scheme have been proposed and analyzed in detail in order to increase the CO_2 capture rate.

2. Process and model description

A detailed layout of the different stages considered for the Ca-Cu process is shown in Fig. 2. As briefly explained in the introduction section, the first stage of the process (indicated as A in Fig. 2) consists of the production of a H_2-rich gas stream at high pressure (stream #5) through the SER process (i.e. combinations of reactions (1), (2) and (3)) using natural gas as feedstock. The natural gas fed into this step is first pre-reformed with steam in an adiabatic pre-reformer working with an inlet temperature of 490 °C (stream #2), and the outlet stream is subsequently heated up to the inlet temperature of stage A ($T_{g,in,A}$, stream #4 in Fig. 2). Pre-reforming of the natural gas is introduced in order to decompose the higher hydrocarbons present in the gas, avoiding in this way their degradation into coke inside the fixed bed reactor. The amount of steam used in this first stage of the Ca-Cu process is controlled through the steam-to-carbon (S/C) molar ratio, which is one of the variables analyzed further on in this work. Stage A finishes when all the active CaO available in the solid bed has been converted into $CaCO_3$.

The next stage of the Ca-Cu process starts when pressurized diluted air is fed to the packed bed reactor (stream #6), which operates at high pressure. Oxidation of the Cu present in the solid bed to CuO occurs, according to the following reaction:

$$Cu + \frac{1}{2}O_2 \rightarrow CuO, \quad \Delta H_{298K} = -156\ \text{kJ/mol} \tag{4}$$

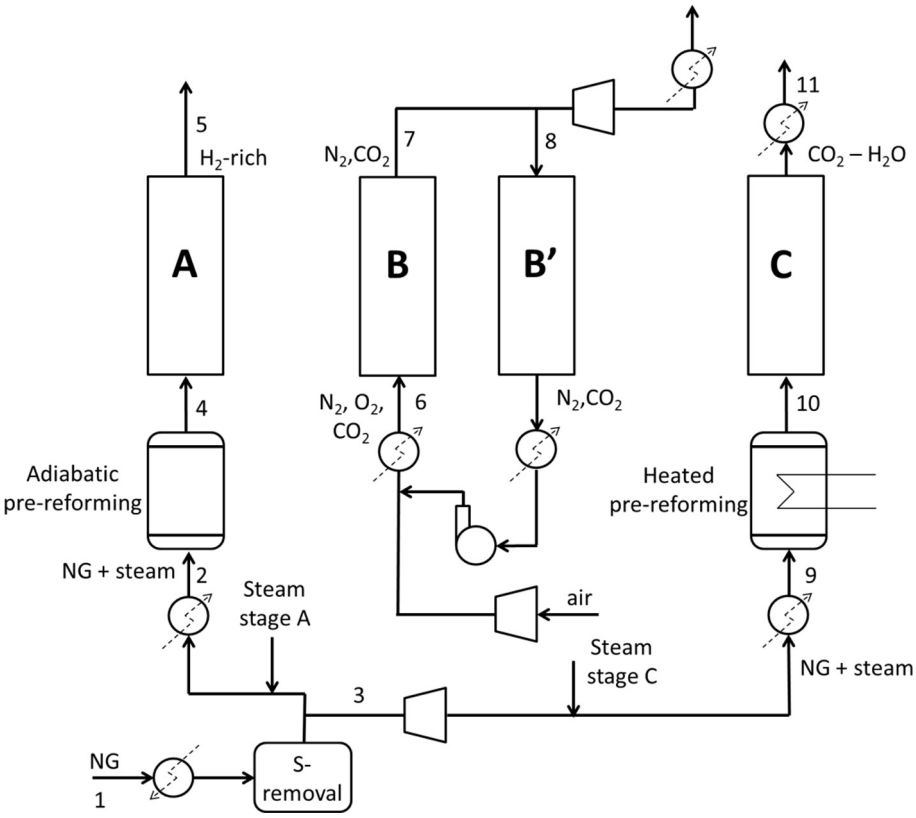

Fig. 2. Process scheme of the Ca-Cu looping process considered in this work.

Due to the high exothermicity of this reaction, it is important to control the maximum temperature reached during this stage ($T_{max,B}$) in the solid bed. Previous analyses carried out by Fernandez et al. [25,26] have demonstrated that $T_{max,B}$ can be kept in a reasonable range of values between 830 and 850 °C by limiting the temperature and the O_2 concentration of the diluted air fed to this stage to very low values (i.e. $T_{gin,B}$ of 300–350 °C and 3–4 vol% of O_2, respectively). A fraction of the O_2-depleted gas at the outlet of stage B is recycled back to the inlet of this stage B to achieve the low O_2 concentration needed (stream #8). Since the gas at the outlet of stage B is at a very high temperature and the solid bed will remain at the temperature of $T_{g,in,B}$ at the end of this stage, as it can be seen from our previous study [22], an intermediate stage B' is added between stages B and C with the aim of cooling down the O_2-depleted recycle before being mixed with the compressed air, as appreciated in Fig. 2. Moreover, in this way the solid bed is heated up to a proper temperature, which allows the reactions to start in the next stage C.

In the last stage of the process, the calcination of the $CaCO_3$ (Eq. (5)) takes place thanks to the heat provided by the reduction of the CuO present in the solid bed when feeding a fuel gas containing H_2, CO and CH_4 (Eqs. (6)–(8) respectively).

$$CaCO_3 \leftrightarrow CaO + CO_2, \quad \Delta H_{298K} = 178\ \text{kJ/mol} \tag{5}$$

$$CuO + H_2 \rightarrow Cu + 3H_2O, \quad \Delta H_{298K} = -86\ \text{kJ/mol} \tag{6}$$

$$CuO + CO \rightarrow Cu + CO_2, \quad \Delta H_{298K} = -127\ \text{kJ/mol} \tag{7}$$

$$4CuO + CH_4 \rightarrow Cu + CO_2 + H_2O, \quad \Delta H_{298K} = -170\ \text{kJ/mol} \tag{8}$$

In order to allow the calcination reaction to occur at reasonable temperatures (about 870 °C), this stage is carried out at atmospheric pressure. To control the maximum temperature in stage C ($T_{max,C}$) the Cu/CaO molar ratio in the solids has to be selected based on the inlet gas composition and the different heats of reaction for Eqs. (6)–(8). Fernandez et al. [25] proposed to feed H_2 and CO at 870 °C coming from an additional step that acts as reformer and cools down the bed before the SER stage. In this work the gas fed (stream #10) is coming from a heated pre-reformer at 700 °C. In this way, since the inlet gas is at equilibrium, no SMR and WGS occur after the solid is regenerated and the temperature at the end of the step remains equal to the one of the inlet gas, making an extra step before stage A unnecessary. If the inlet gas is not in equilibrium (i.e. when coming from an adiabatic pre-reformer), SMR and WGS reactions start to take place as soon as it enters the reactor and the temperature inside the bed decreases to the equilibrium temperature of the gas. The low temperature reached in the bed at the beginning of stage A could favor the hydration of CaO, because the gas is at high pressure and with a high concentration of steam. The possibility of the formation of liquid eutectics in the system $CaO/Ca(OH)_2/CaCO_3$ or the effect of $Ca(OH)_2$ formation on the performance of the solids or the SER equilibrium was discussed by Martínez et al. [19]. To avoid the adverse effects on sorbent particles (breakage and formation of melts) caused by CaO hydration [27,28], operating conditions in the Ca-Cu process have been selected so that $Ca(OH)_2$ formation is avoided according to thermodynamics.To study this process the 1-D pseudo-homogeneous model (PHM) described in a previous work [22] has been used. An overview of the mass and energy balances solved by the PHM is given in Table 1. In this model it is assumed that the reactor is an adiabatic packed bed reactor, which means that no heat losses through the reactor wall are considered. No radial temperature and concentration gradients are considered and mass and heat transfer resistances between the gas and solid phases are neglected, resulting in a negligible temperature difference between both phases along the reactor. Axial mass dispersion

Table 1
Mass and energy balances solved in the 1D pseudo-homogeneous model.

Component mass balances for the gas phase:

$$\frac{\partial}{\partial t}\left(\varepsilon_g \rho_g \omega_{i,g}\right) = -\frac{\partial}{\partial x}\left(\rho_g v_g \omega_{i,g}\right) + \frac{\partial}{\partial x}\left(\rho_g D_{ax}\frac{\partial \omega_{i,g}}{\partial x}\right) + \varepsilon_g r_i M_i$$

Component mass balances for the solid phase:

$$\varepsilon_s \rho_s \frac{\partial \omega_{i,s}}{\partial t} = \varepsilon_g r_i M_i$$

Energy balance:

$$(\varepsilon_g \rho_g C_{p,g} + \varepsilon_s \rho_s C_{p,s})\frac{\partial T}{\partial t} = -\rho_s v_g C_{p,g}\frac{\partial T}{\partial x} + \frac{\partial}{\partial x}\left(\lambda_{eff}\frac{\partial T}{\partial x}\right) + \varepsilon_g r_i \Delta_r H$$

Momentum balance (Ergun equation, [43])

$$\frac{dP}{dx} = -150\frac{v_g(1-\varepsilon_g)^2}{d_p^2\varepsilon_g^3} + 1.75\frac{v_g^2(1-\varepsilon_g)}{d_p\varepsilon_g^3}$$

Reaction rates:

Steam methane reforming and water gas shift (from Numaguchi and Kikuchi [29]):

$$r_1 = \eta A_1 e^{\frac{-E_{act,1}}{RT}}\left(\frac{p_{CH_4}p_{H_2O} - \frac{p_{CO}p_{H_2}^3}{K_1}}{p_{H_2O}^{1.596}}\right),\ r_2 = \eta A_2 e^{\frac{-E_{act,2}}{RT}}\left(\frac{p_{CO}p_{H_2O} - \frac{p_{CO_2}p_{H_2}^3}{K_2}}{p_{H_2O}}\right)$$

Carbonation and calcination (from Li and Cai [30] and Martinez at al. [31], respectively):

$$r_i = \eta\frac{\rho_i}{M_w^i}A_i e^{\frac{-E_{act,i}}{RT}}(1-X)^{2/3}\left(c_{CO_2} - \frac{p_{CO_2}^{eq}}{RT}\right)\left(\frac{p}{p_0}\right)^{-q_p}$$

Oxidation and reduction (from Hamers et al. [32] and Medrano et al. [33]):

$$r = \eta k_0 e^{\frac{-E_{act}}{RT}}c_i^n\left(\frac{p}{10^5}\right)^{-q_p}$$

and effective heat conductivity are taken into account in the mass and heat balances and the closure equations are listed in Table 2. Concerning the kinetic expressions considered in the model for the different reactions occurring in the process, different reaction models have been taken from literature as indicated in Table 1 (i.e. expressions from Numaguchi and Kikuchi [29] for the SMR and WGS reactions, from Li and Cai [30] and Martínez at al. [31] for carbonation and calcination, respectively, and from Hamers et al. [32] for the oxidation/reduction of the Cu-based material and Medrano et al. [33] for the oxidation/reduction of the catalyst). In order to account for the internal diffusion resistance into the kinetics an effectiveness factor (η) was considered for all the reactions. For the SMR and WGS η was calculated in the model using the Thiele modulus (Φ, Eq. (9)) and a value of around 0.8 for both reactions was found. For the carbonation reaction an effectiveness factor of 0.3 was used according to Fernandez et al. [34] while for the calcination reaction and the oxidation and reduction reactions an effectiveness factor of around 0.8 was considered [32].

$$\eta = \frac{\tanh(\Phi)}{\Phi} and \Phi = L\sqrt{\frac{k}{D_{eff}}} \tag{9}$$

In this case, simulations have been performed taking into account that in addition to the Ca-based sorbent and the Cu-based material, a reforming Ni-based catalyst is present in the bed. For these calculations the following solid compositions have been considered: a CaO-based material (CO_2 sorbent) with 85%wt of CaO (30% active) on Al_2O_3 [35–38], an oxygen carrier with 65% wt of Cu over Al_2O_3 [4,39] and a Ni-based reforming catalyst containing 18%wt. of Ni on Al_2O_3[40]. A Cu/CaO molar ratio of 1.7 (given per mole of active CaO) was calculated from the enthalpies of the reactions occurring in step C in order to have an energy neutral operation of this step at $T_{max,C}$. A catalyst-to-sorbent mass ratio of 0.3 was chosen following the work of Fernandez et al. in order to achieve a high H_2 purity in the product gas of step A (SER) [34].

Table 2
Equations for the description of heat and mass dispersion.

Effective axial heat dispersion (Vortmeyer and Berninger [44]):

$$\lambda_{eff} = \lambda_{bed,0} + \frac{\mathrm{RePr}\lambda_g}{Pe_{ax}} + \frac{\mathrm{Re}^2\mathrm{Pr}^2\lambda_g}{6(1-\varepsilon_g)\mathrm{Nu}}$$

Gunn and Misbah equation [45]:

$$\mathrm{Pe}_{ax} = \frac{2(0.17+0.33\exp(-24/\mathrm{Re}))}{1-(0.17+0.33\exp(-24/\mathrm{Re}))}$$

Gunn equation [46]:

$$\mathrm{Nu} = (7-10\varepsilon_g+5\varepsilon_g^2)(1+0.7\mathrm{Re}^{0.2}\mathrm{Pr}^{1/3}) + (1.33-2.4\varepsilon_g+1.2\varepsilon_g^2)\mathrm{Re}^{0.7}\mathrm{Pr}^{1/3}$$

Axial mass dispersion (Edwards and Richardson [47]):

$$D_{ax} = \left(\frac{0.73}{\mathrm{ReSc}} + \frac{0.5}{\varepsilon_g + \frac{9.7\varepsilon_g^2}{\mathrm{ReSc}}}\right)v_g d_p$$

Since the objective of this work is to optimize the operating conditions of the process in order to increase the CO_2 capture rate, the main parameter used to compare the different cases studied is the carbon capture efficiency, which has been defined as follows depending on whether it is calculated considering exclusively the SER stage (CCE_{SER}) or the complete process (CCE_{tot}):

$$CCE_{SER} = \left(1 - \frac{n_{C,out,SER}}{n_{C,in,SER}}\right) \times 100 \tag{10}$$

$$CCE_{tot} = \left(1 - \frac{n_{C,out}}{n_{C,in}}\right) \times 100 \tag{11}$$

where $n_{C,in,SER}$ and $n_{C,out,SER}$ are, respectively, the number of moles entering and exiting the SER stage and $n_{C,in}$ and $n_{C,out}$ are the number of moles entering the system (SER stage and step C) and total number on moles of carbon lost from the process (step A and step B-B′).

3. Results and discussion

3.1. Base case: reference operating conditions

Simulations with the PHM have been performed for the different stages of the Ca-Cu process shown in Fig. 2, using the reference set of operating conditions listed in Table 3. The mass flow rate entering stage A was selected in order to have a gas velocity at the entrance of the reactor of 0.5 m/s. The mass flow rate in stages B and B' was chosen to make the steps last twice the time of stage A, in order to limit the pressure drop (i.e. with an inlet gas velocity of 1.3 m/s the pressure drop is around 15%) since the amount of diluted air needed to oxidize the bed is very high, while the mass flow rate in stage C was chosen to make the step last the same time

Table 3
Natural gas properties and operating conditions of the reference case.

Natural gas properties	
CH_4 – Methane [%mol]	89.00
C_2H_6 – Ethane [%mol]	7.00
C_3H_8 – Propane [%mol]	1.00
C_4H_{10} – Butane [%mol]	0.11
CO_2, [%mol]	2.00
N_2, [%mol]	0.89
Molar mass, kg/kmol	18.018
Lower Heating Value, MJ/kg	46.482
Higher Heating Value, MJ/kg	51.454
Operating condition of the reference case	
Reactor diameter [m]	4.5
Reactor length [m]	10
Particle size [m]	0.01
Inlet temperature at the HP adiabatic pre-reformer [°C]	490
Steam-to-carbon molar ratio at HP adiabatic pre-reformer inlet	3
Inlet temperature at LP heated pre-reformer [°C]	490
Steam-to-carbon molar ratio at LP heated pre-reformer inlet	1
Inlet gas velocity in stage A [m/s]	0.5
Mass flux entering stage A [kg/m^2/s]	2.67
Feed gas temperature to stages A [°C]	700
Feed gas temperature to stage B [°C]	340
Feed gas temperature to stage C [°C]	700
Operating pressure of stage A [bar]	25.2
Operating pressure of stage B [bar]	21
Operating pressure of stage C [bar]	1.8
Molar fraction of O_2 at stage B inlet [%]	3

as stage A. Fig. 3a shows the axial temperature profile inside the bed at the beginning of stage A that corresponds to the final temperature profile of step C, where the two parts of the bed at different temperatures ($T_{s0,1}$ and $T_{s0,2}$) can be appreciated. Fig. 3b–d show the axial temperature, the solid and the gas composition profiles inside the bed at an intermediate time during the first stage of the Ca-Cu process. As shown in Fig. 3b, the solid bed cools down below the inlet gas temperature ($T_{g,in,A}$) in the first part of the bed, reaching a temperature of T_{ad}. The solids in this part of the bed do not have active CaO available that can react with the formed CO_2 since it has already been carbonated (see the conversion of the CaO in Fig. 3c), and therefore only reforming and WGS reactions can occur, promoted by the presence of the Ni-based catalyst. Due to the fact that the pre-reformer placed upstream of stage A operates adiabatically with an inlet temperature of 490 °C, the gas fed to the solid bed is not at equilibrium at $T_{g,in,A}$. Consequently, as gas is fed to the reactor, it reacts according to the reforming and WGS reactions thanks to the sensible heat

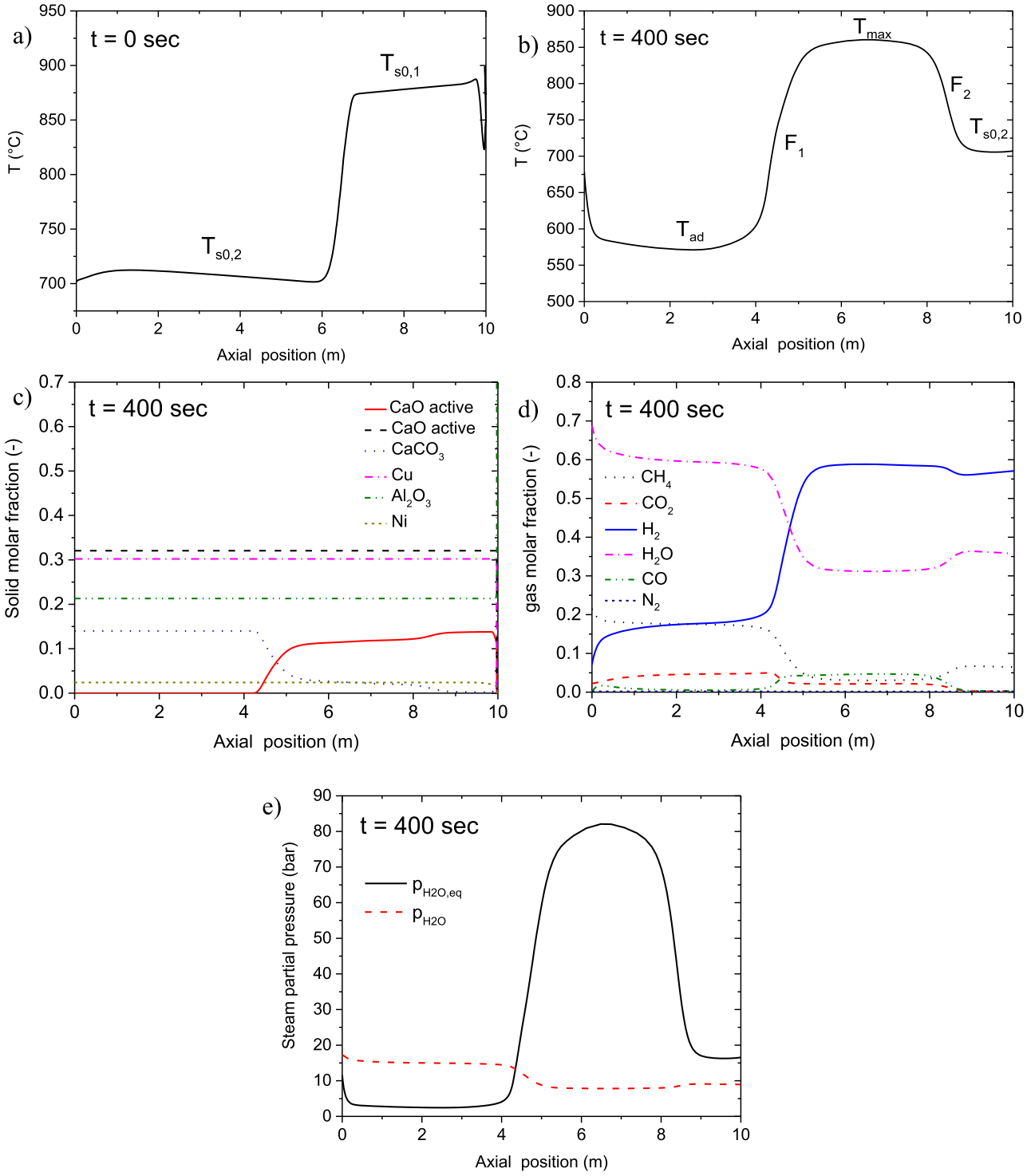

Fig. 3. Axial temperature profiles at the beginning of stage A (a) and axial temperature (b), solid composition (c), gas composition (d) and steam partial pressure (e) profiles along the bed at an intermediate time during stage A under the conditions of the reference case.

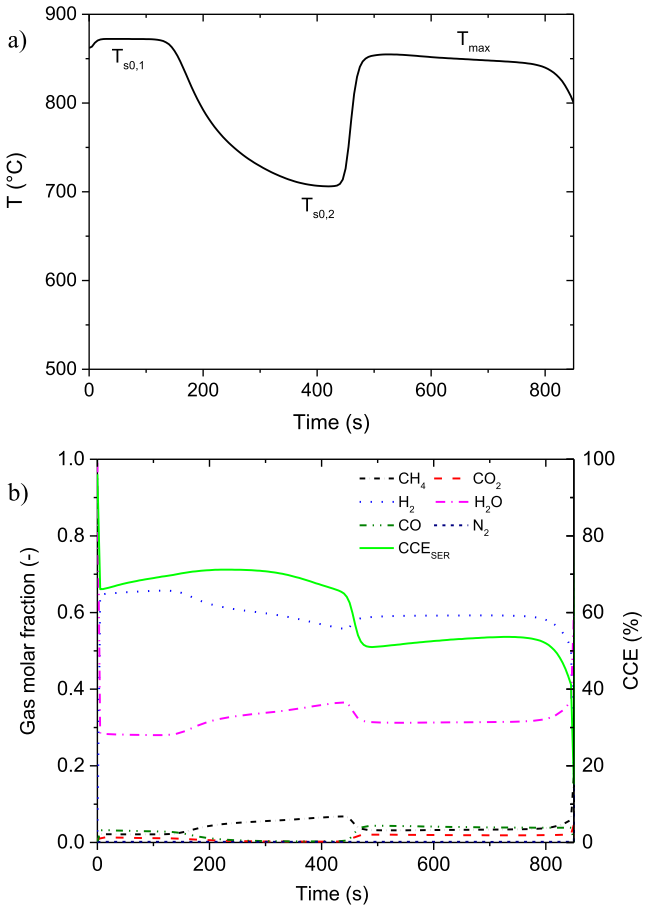

Fig. 4. Temperature (a) and gas composition and carbon capture efficiency (b) of the outlet stream from stage A as a function of time for the reference case.

stored in the solids, causing the solid bed temperature to decrease to T_{ad}. When the gas reaches the part of the solid bed where there is active CaO available (i.e. after crossing the front F_1 indicated in Fig. 3b), the carbonation reaction starts to take place and the temperature increases until the maximum temperature $T_{max,A}$ of around 850 °C is reached. At this $T_{max,A}$, the carbonation reaction proceeds very slowly due to thermodynamic restrictions, being boosted again downstream in the solid bed when the temperature decreases to the initial bed temperature $T_{s0,2}$ of 707 °C (i.e. right hand side of front F_2 in Fig. 3b). In order to check if hydration could occur inside the reactor the equilibrium partial pressure was calculated along the bed according to Eq. (12) [41] and compared with the steam partial pressure present in the bed as shown in Fig. 3e. It can be seen that in the first part of the bed there is the condition for the hydration to happen since the steam partial pressure is higher than the equilibrium partial pressure. However, in this region all the CaO is already completely carbonated so no hydration is expected to occur. In the second part of the bed, where the CaO is still present in the bed, the equilibrium partial pressure is much higher than the steam partial pressure, meaning that no hydration will occur. From these results it can be assumed that no hydration will occur in the bed during stage A.

$$p_{H_2O,eq} = 2.30 \times 10^8 \exp\left(-\frac{11607}{T}\right) \quad (12)$$

The presence of the heat plateau at such high temperature $T_{max,A}$ inside the solid bed is substantially due to the fact that reforming and carbonation reactions do not completely occur at the same reaction front, but reforming is initiated before the carbonation starts. Therefore, the reforming process does not completely absorb the energy released from the carbonation reaction, as expected in a completely mixed fluidized bed SER reactor. The consequent temperature increase within the carbonation reaction front limits CO_2 absorption and thus the carbon capture efficiency (CCE) that can be reached. Hence, in the part of the bed at $T_{max,A}$ between fronts F_1 and F_2, the amount of CO and CO_2 in the gas phase increases as can be appreciated from the gas concentration profiles along the bed shown in Fig. 3d.

Step A should finish when all the active CaO present in the solid bed is in the form of $CaCO_3$, that is when the front F_1 reaches the end of the reactor. It is important that there is no active CaO available at the end of stage A, since the heat released by CuO reduction during the regeneration stage may lead to temperature peaks along the bed that could result into agglomeration or undesired reactions of the Cu-based material. When stage A finishes, the entire solid bed is practically at a constant temperature T_{ad}. However, the gas exiting the solid bed during the whole duration of stage A does

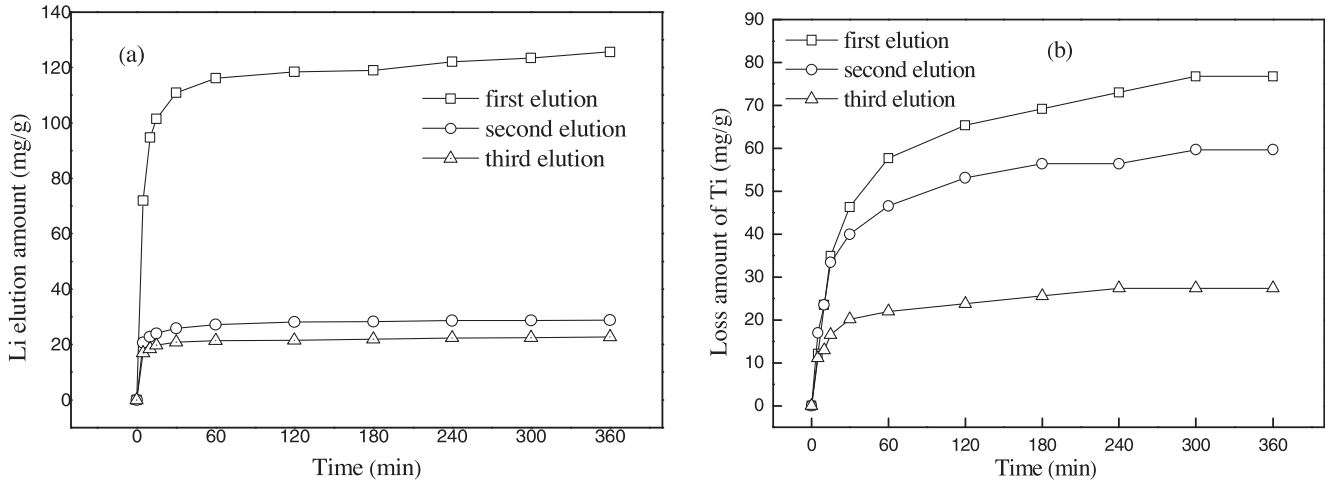

Fig. 5. Carbon capture efficiency (CCESER), conversion of CH_4, CO and CO_2 as a function of pressure (a), S/C ratio (b), initial bed temperature (c), inlet gas temperature (d) and productivity under the following conditions: a) S/C = 3, $T_{g,in,A} = T_{s,0} = 700$ °C and inlet gas from adiabatic pre-reforming at 490 °C; b) P = 25 bar, $T_{g,in,A} = T_{s,0} = 700$ °C and inlet gas from adiabatic pre-reforming at 490 °C; c) P = 25 bar, S/C = 5, $T_{g,in,A} = 700$ °C and feed gas from adiabatic pre-reforming with inlet temperature of 490 °C; d) P = 25 bar, S/C = 5, $T_{s,0} = 700$ °C and feed gas from adiabatic pre-reforming with inlet temperature of 490 °C.

not have a constant temperature and composition, as shown in Fig. 4.

During the first 450 s, before the first front F_2 reaches the end of the reactor, the H_2- rich gas exiting the solid bed reactor is at two different temperatures of $T_{s0,1}$ = 880 °C and $T_{s0,2}$ = 707 °C with a low content of carbon compounds (~6% of CO, CO_2 and CH_4). Carbon slip is relatively low during this period and a relatively high CCE_{SER} of around 71% is achieved. However, as it can be appreciated in Fig. 4, during the second period of time the gas starts exiting from the solid bed at $T_{max,A}$ = 850 °C and the amount of carbon compounds in the H_2-rich gas increases, which causes a decrease in the CCE_{SER} to 53% (considering the operating period between 450 s and 850 s, before the breakthrough). After 850 s a third period corresponds to the breakthrough time, in which the CCE_{SER} is decreasing very fast to zero. All this contributes to a reduction in the overall CCE_{SER} achieved in stage A to around 61%. The loss in the breakthrough time could be reduced by decreasing the velocity of the gas and thus increasing the sharpness of the profiles. However, the decrease in the gas superficial velocity would result in larger reactor volumes and so in an increase of the corresponding capital costs.

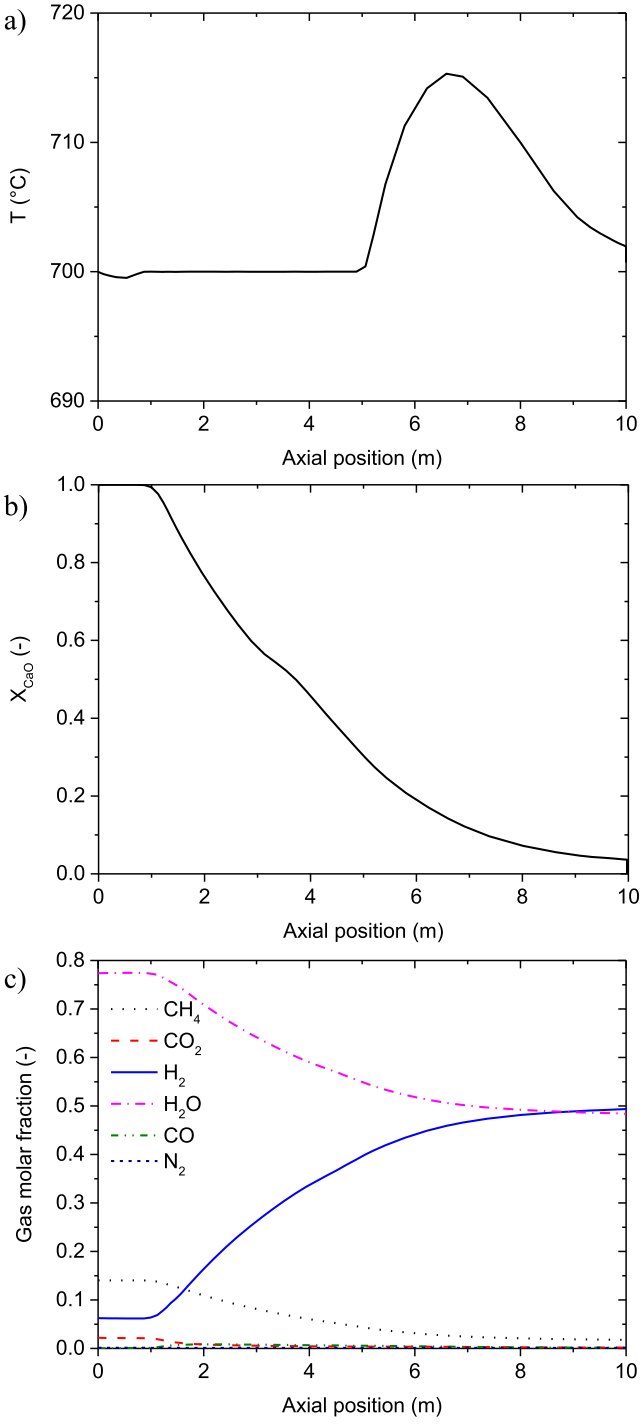

Fig. 6. Axial temperature (a), active CaO conversion (b) and gas (c) profiles inside the bed after 400 s of stage A for the case with no reforming under 700 °C; P = 25 bar, S/C = 5, $T_{g,in,A}$ = $T_{s,0}$ = 700 °C.

3.2. Sensitivity analysis on stage A operating parameters

A sensitivity analysis on the performance of step A has been carried out in order to understand the influence of the different operating conditions on the CCE achieved in this stage of the Ca-Cu process. Different simulations with the 1-D PHM have been performed varying the following operating conditions: pressure, initial bed temperature ($T_{s,0}$), inlet gas temperature ($T_{g,in,A}$) and steam-to-carbon (S/C) ratio. For these analyses, an initial flat temperature profile in the bed (i.e. entire solid bed at $T_{s,0}$) was considered to reduce calculation time of the PHM, which has been run exclusively for stage A conditions. As demonstrated from the results shown in this analysis, the CCE obtained for stage A is not significantly influenced by the shape of the initial bed temperature profile. In particular, the CCE_{SER} of step A of the reference case changes from 61% when calculated with the rigorous initial temperature profile of Fig. 3a, to 61.5% when calculated with a uniform initial temperature equal to $Ts_{0,2}$. To analyze the results, the con-

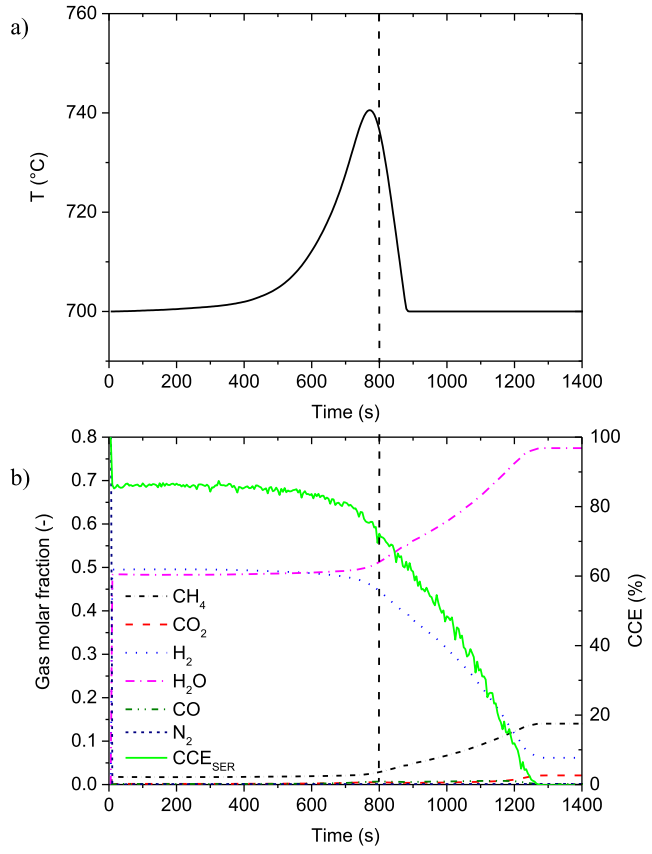

Fig. 7. Temperature (a), composition and carbon capture efficiency (b) of the outlet gas stream of stage A in the case with no reforming under 700 °C; P = 25 bar, S/C = 5, $T_{g,in,A}$ = $T_{s,0}$ = 700 °C.

versions of CH_4, CO and CO_2, calculated according to Eq. (13)–(15), respectively, have been monitored.

$$\eta_{CH_4} = 1 - \sum_i \frac{\dot{n}_{tot,out,i}}{\dot{n}_{tot,in}} \frac{y_{CH_4,out,i}}{y_{CH_4,in}} \frac{\Delta t}{t_{step}} \quad (13)$$

$$\eta_{CO} = 1 - \sum_i \frac{\dot{n}_{tot,out,i}}{\dot{n}_{tot,in}} \frac{y_{CO,out,i}}{y_{CO,in} + y_{CH_4,in} \cdot \eta_{CH_4}} \frac{\Delta t}{t_{step}} \quad (14)$$

$$\eta_{CO_2} = 1 - \sum_i \frac{\dot{n}_{tot,out,i}}{\dot{n}_{tot,in}} \frac{y_{CO_2,out,i}}{y_{CO_2,in} + y_{CO,in} \cdot \eta_{CO} + y_{CH_4,in} \cdot \eta_{CH_4} \cdot \eta_{CO}} \frac{\Delta t}{t_{step}} \quad (15)$$

In Fig. 5a the CCE_{SER} and the conversion of CH_4, CO and CO_2 as a function of the total pressure are plotted. The operating pressure has been varied between 15 and 30 bar while maintaining the other operating conditions of stage A equal to those of the reference case (see Table 3). As the figure shows, the operating pressure of stage A does not have a pronounced influence on the CCE reached in this stage, remaining almost constant over the range of values investigated. When reducing the pressure, the conversion of CO and CH_4 increases, while for the CO_2 conversion the opposite trend is observed. When the pressure is varied, these effects compensate each other resulting in a minimal effect on the CCE_{SER}. Considering that the application envisaged in this work for the Ca-Cu process is on power production (i.e. using the H_2-rich gas produced as fuel in the gas turbine of a combined cycle), a pressure of the H_2-rich stream around 25–30 bar is needed at the outlet of stage A. Increasing too much the pressure in stage A above these values would increase the probability of $Ca(OH)_2$ formation. Lower pressures than 25–30 bar would reduce the risk of $Ca(OH)_2$ formation, but an additional compression step for the H_2-rich gas produced to be fed to the gas turbine would be needed. Based on these facts, a reasonable pressure value of 25 bar has been selected for stage A, which was kept constant in the following analyses.

To assess the effect of the S/C ratio, simulations have been performed with S/C between 3 and 5. Two sets of simulations were performed for two different values of the initial bed temperature ($T_{s,0}$) and inlet gas temperature ($T_{g,in,A}$) of 650 °C and 700 °C. In Fig. 5b the CCE and CH_4, CO and CO_2 conversions are plotted as a function of the S/C ratio for the case with $T_{s,0} = T_{g,in,A} = 700$ °C. It can be seen that when increasing the S/C ratio at stage A inlet, the CCE_{SER} increases. The same trend is also noticed for the conversion of CH_4, while the CO and CO_2 conversions remain almost constant for different S/C. This is due to the fact that increasing the amount of steam in the gas enhances the CH_4 conversion through the reforming reaction (Eq. (1)), producing more CO_2 that is ultimately separated from the gas phase through the reaction with CaO (Eq. (3)). The same behavior was found for the case with $T_{s,0} = T_{g,in,A} = 650$ °C (which is not reported in Fig. 5 for brevity). Since from this study an S/C ratio of 5 was found to give the highest CCE, this value was kept for the following analyses.

Another important parameter studied is the initial solid bed temperature at the beginning of stage A ($T_{s,0}$), which has been varied between 650 °C and 800 °C. Simulations were performed considering a $T_{g,in,A}$ of 700 °C. In Fig. 5c the CCE_{SER} and the conversion of CH_4, CO and CO_2 are plotted as a function of $T_{s,0}$. It can be seen that the CCE reaches a maximum value of 74 % for $T_{s,0} = 700$ °C. Increasing the $T_{s,0}$ above this value enhances the CH_4 conversion through the reforming reaction. On the other hand, the WGS and carbonation reactions are favored at low temperature, which makes the conversions of CO and CO_2 increase when reducing the temperature. At lower temperatures, the CCE_{SER} is limited by the CH_4 conversion by the SMR reaction (CH_4 conversion and CCE have the same trend below 700 °C in Fig. 5c). The best compromise between these two opposite effects at the selected

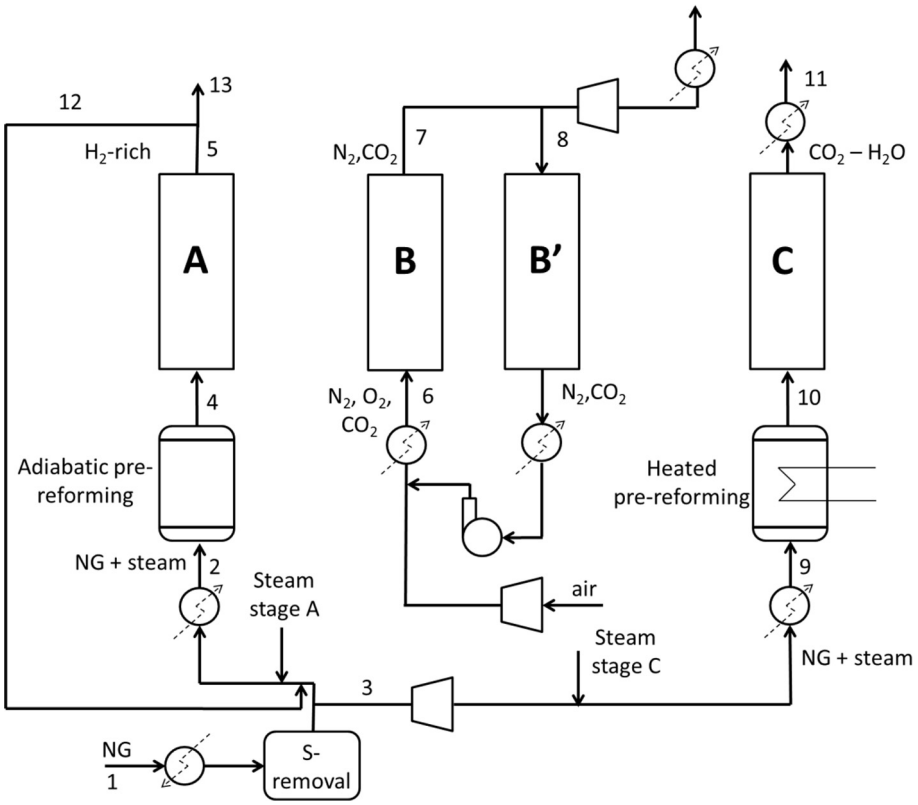

Fig. 8. Scheme of the Ca-Cu process with H2-rich stream recycle in stage A.

pressure and S/C is found at an initial bed temperature $T_{s,0}$ of 700 °C.

The influence of the inlet gas temperature to stage A ($T_{g,in,A}$) was also studied, modifying its value in the range 500–700 °C. In Fig. 5d the CCE_{SER} and the conversion of CH_4, CO and CO_2 are plotted as a function of $T_{g,in,A}$. When lowering the $T_{g,in,A}$, the reforming reaction at the initial part of the bed is less favored, resulting in a higher amount of CH_4 in the gas reaching the part of the bed where active CaO is available. In this way, since the reforming of CH_4 acts as a heat sink in the reaction system, the amount of heat released in this section of the bed due to SER reactions is lower, and so the temperature plateau at $T_{max,A}$ becomes shorter. Moreover, the carbonation and WGS reactions are favored at lower temperatures (T_{ad} decreases with $T_{g,in,A}$) and therefore CO and CO_2 are consumed by the two reactions favoring the equilibrium of the SMR. Oppositely, as confirmed by the results plotted in Fig. 5d, the CO and CO_2 conversions decrease when increasing the inlet gas temperature. For temperatures higher that 575 °C the CCE_{SER} follows the same trend than the conversion of CO and CO_2, increasing by decreasing the inlet temperature, while for lower temperatures the low conversion of CH_4 is the limiting factor. This is due to the fact that decreasing the temperature the SMR kinetics become really slow compared to the gas velocity and therefore the residence time is too low. This could be improved by decreasing the inlet flow rate and therefore the productivity, but then the cycle time would increase and more reactors would be needed. As can be seen from Fig. 5e, by decreasing the productivity the CCE increases due to the increase in CH_4 conversion, reaching a maximum of 80%, which is not much higher than the 78% found with an inlet temperature of 575 °C.

As the initial bed temperature reduces, the conditions for the formation of hydrates could be attained in the first part of the bed at T_{ad}. However, in this part of the bed, only $CaCO_3$ is present when reaching the temperature T_{ad}, which should prevent the reaction of the sorbent with steam.

From the point of view of CCE_{SER}, the best operating conditions for stage A found from this sensitivity analysis correspond to a pressure of 25 bar, a S/C ratio of 5 at the pre-reformer inlet, an initial bed temperature $T_{s,0}$ of 700 °C and an inlet gas temperature $T_{g,in,A}$ of 575 °C. For these conditions, a CCE in stage A of around 78% was found. A complete cycle was simulated with these new operating conditions in stage A while for the other stages the same operating conditions as the reference case were chosen. For this case an overall carbon capture efficiency (CCE_{tot}) of around 82% was found, that is still rather limited compared to alternative CO_2 capture technologies for combined cycle power plants.

3.3. Characteristics of an ideal catalyst

As discussed above, the main problem of the low CCE during stage A of the Ca-Cu process is associated with the high temperature plateau that is formed inside the bed during this step, caused by the decoupling of the SMR and the carbonation reaction fronts.

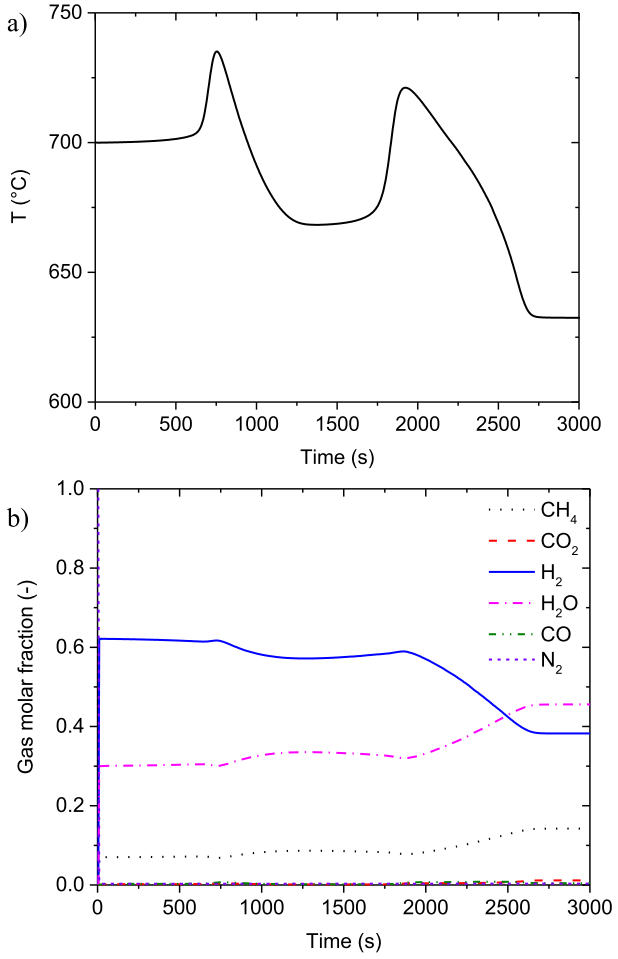

Fig. 9. Temperature (a) and composition (b) of the outlet gas stream of stage A for the case with a H2-rich stream recycle; P = 20 bar, S/C = 3, $T_{g,in,A} = T_{s,0} = 700$ °C.

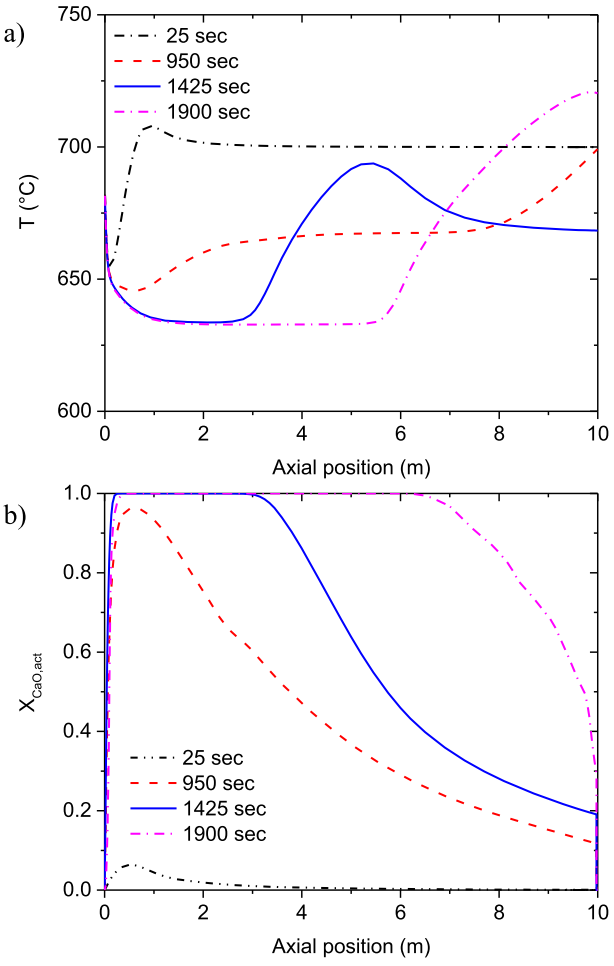

Fig. 10. Axial temperature (a) and active CaO conversion (b) profiles inside the bed during step A for the case with a H2-rich stream recycle at different moments in time. P = 20 bar, S/C = 3, $T_{g,in,A} = T_{s,0} = 700$ °C.

A way to decrease the maximum temperature reached in the bed is to consider an ideal reforming catalyst inactive under 700 °C, so that limited advancement of the SMR reaction occurs in the first part of the bed already carbonated. In this case, the bed temperature in the first part of the bed cannot decrease below 700 °C because of SMR, and most of the reforming would occur at the same reaction front of the carbonation reaction. As a consequence, a lower value of $T_{max,A}$ will be reached and a higher advancement of the carbonation reaction is obtained, leading to a higher expected CCE.

For analyzing the performance of the stage A under this assumption, axial temperature and concentration profiles along the bed were calculated with the PHM considering the S/C ratio, the pressure and the initial bed temperature equal to those of the best case from the sensitivity analysis and an inlet gas temperature of 700 °C. Simulations have been performed considering that below 700 °C the activity of the ideal reforming catalyst is so low that the reforming reaction does not occur (i.e. SMR kinetic constant $r_1 = 0$). In Fig. 6 the axial temperature and concentration profiles inside the bed are shown. As can be appreciated, all the reactions (carbonation, SMR and WGS) take place at the same front and just one temperature peak is present due to the different rates of the reactions involved. The temperature rise in the bed is much lower than in the reference case (c.f. Fig. 3), reaching in this case a maximum value of around 715 °C. In the first part of the bed, when all CaO has already been carbonated, the temperature remains constant at 700 °C since no reaction occurs, as well as in the last part of the bed (at the right-hand side of the temperature peak) where the bed is at $T_{s,0}$ and it has not been reached yet by the reaction front. In Fig. 7 the composition, CCE_{SER} and temperature of the outlet gas stream of stage A are shown. It can be seen that during the whole duration of the step (that finishes after around 800 s, when the temperature peak, and thus the reaction front, reaches the outlet of the reactor), the gas composition is constant, and this is due to the absence of the high temperature plateau inside the bed. Also the CCE_{SER} is constant during the pre-breakthrough time at a value of around 86% and decreases to zero after the breakthrough.

Although the catalyst used in this calculation is an ideal material, the results obtained from this analysis demonstrate that the low CCE_{SER} observed for the reference case study is largely due to the decoupling of the reforming and carbonation reactions on two different reaction fronts. Consequently, the operation of this Ca-Cu process would greatly benefit from reforming catalysts with rather limited reforming activity below 700 °C, which can open a new research window for this emerging process.

3.4. Alternative Ca-Cu process configurations

As highlighted before, the main issue to overcome the problem of limited CCE in the Ca-Cu process is the high temperature plateau formed inside the bed during stage A of the process. Two new schemes are proposed and explained in the following sections.

3.4.1. Ca-Cu process configuration with H_2-rich stream recycle in stage A

To improve the CCE, the possibility of recycling part of the outlet gas stream of stage A has been investigated in order to dilute the inlet gases to this stage (as shown in Fig. 8). In this way the recycled gas would act as a thermal ballast, and so reduce the value of $T_{max,A}$ reached inside the bed. However, when recycling the outlet gas, the partial pressure of CO_2 in the gas phase along the bed is noticeably decreased and so the carbonation reaction kinetics turns out to become very slow, resulting in a situation where profiles are very broad. In Fig. 9 the temperature and gas composition of the outlet gas stream of stage A are shown for the case with a recycle of 53% of the outlet stream, with a S/C ratio of 3, at 20 bar and 700 °C of $T_{g,in,A}$ and $T_{s,0}$. As it can be seen from the figure, the breakthrough lasts around 700 s, which compared to the total time of the step is quite high. The CCE_{SER} of the first 1900 s is around 62% while the CCE_{SER} calculated considering the break-

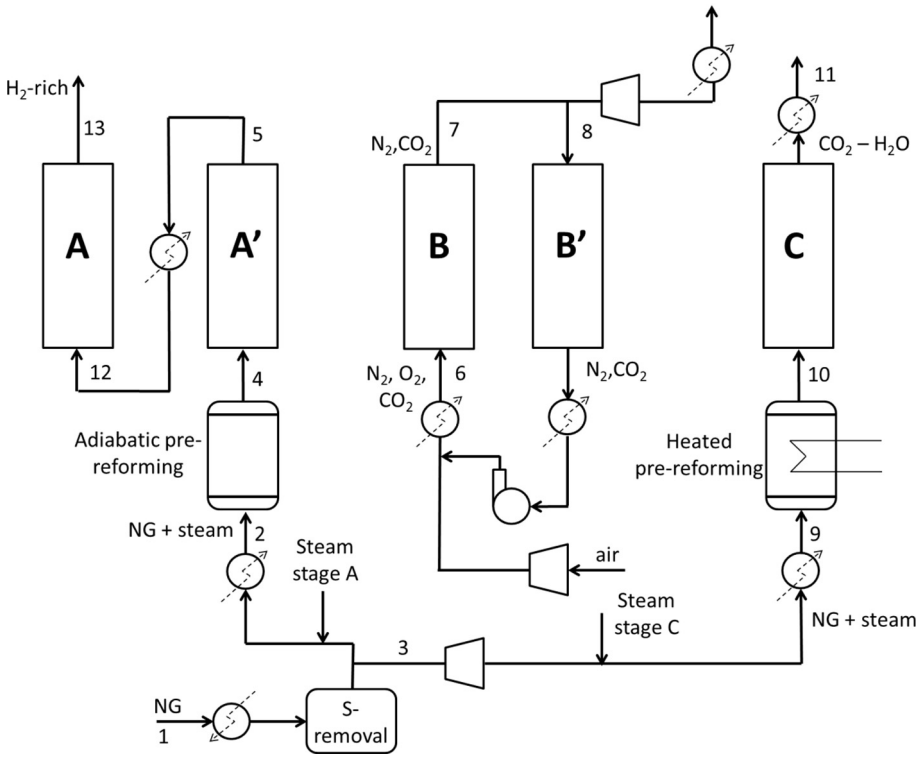

Fig. 11. Scheme of the Ca-Cu process with two beds in series for the SER stage and with intermediate gas cooling.

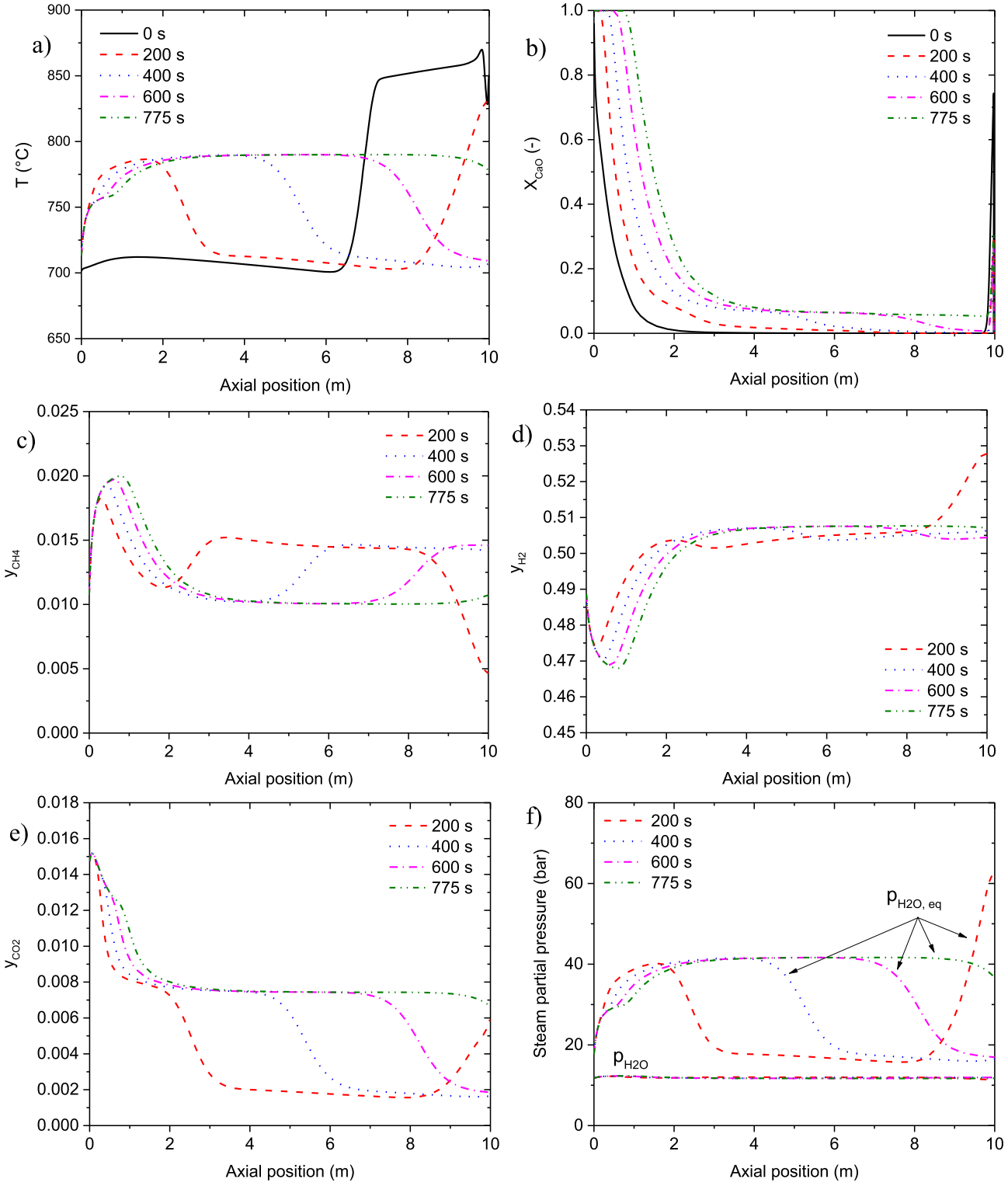

Fig. 12. Axial temperature (a), CaO conversion (b) gas molar fraction (c, d and e) and steam partial pressure (f) profiles inside reactor in stage A at different moments in time.

through time (i.e. 2000 s) is around 59%. If only the gas exiting during the first 1900 s were considered, the CCE_{SER} would be slightly higher than the one of the reference case but part of the bed would not be carbonated. This can be seen in Fig. 10, in which the axial temperature and solid conversion profiles along the bed are plotted. At 1900 s some CaO is still present in the bed, therefore if the step is stopped at this time some CaO would not be used and this may lead to temperature peaks along the bed during the regeneration step (as discussed in Section 3.1). Four different recycles were investigated, but the behavior found was the same and the CCE_{SER} was always around 60%. By increasing the recycle ratio the broadness of the profiles is increased, whereas if the recycle

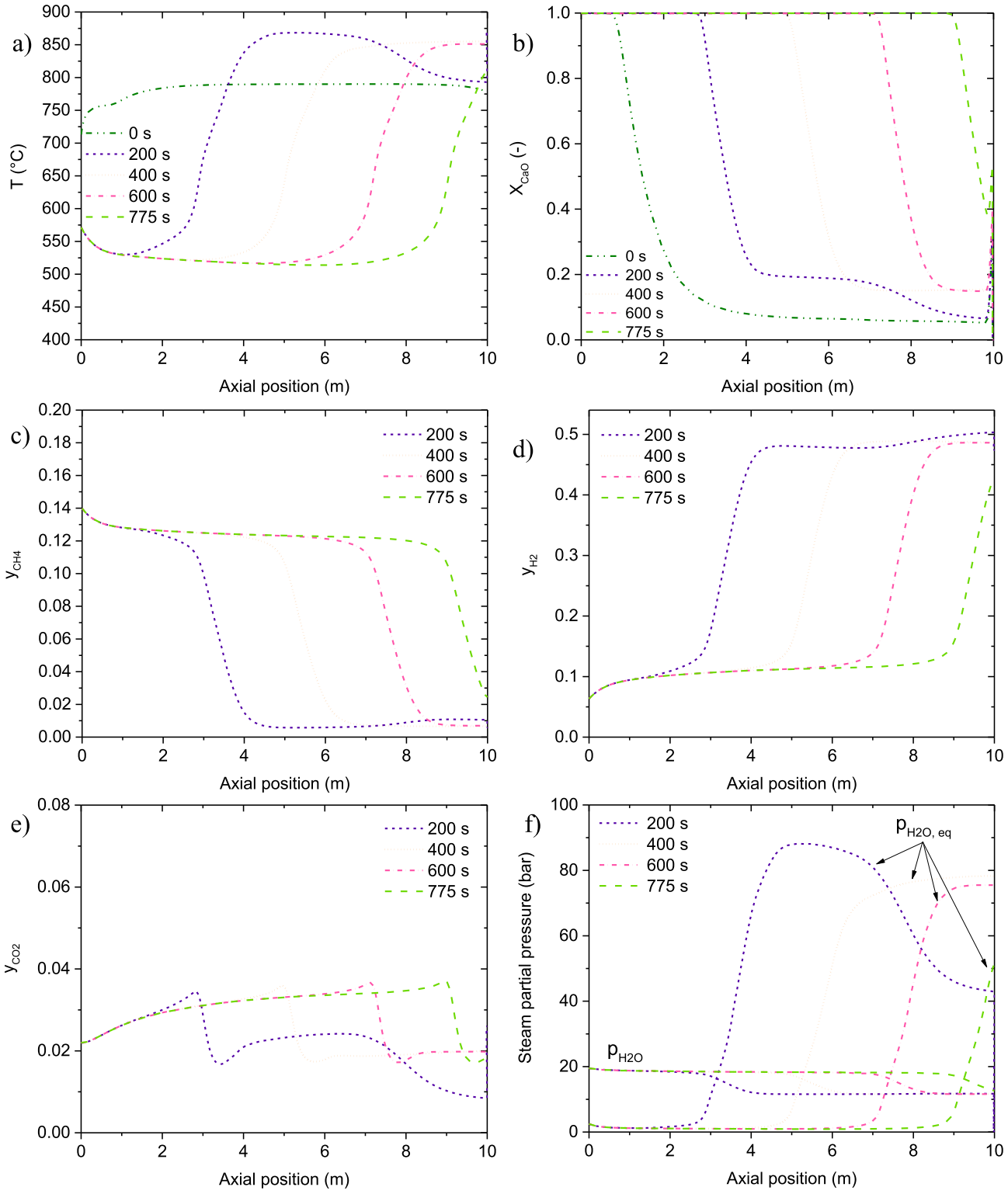

Fig. 13. Axial temperature (a), CaO conversion (b) gas molar fraction (c–e) and steam partial pressure (f) profiles inside reactor in stage A' at different moments in time.

ratio is decreased not much benefit on the CCE is accomplished. An alternative scheme is therefore suggested and explained in the following section.

3.4.2. Ca-Cu process configuration with a two-stage SER with gas intercooling

This scheme is based on splitting the SER step into two stages, named A and A′, according to Fig. 11. In this configuration, the fresh charge (pre-reformed natural gas and steam, stream #4) is sent to reactor in stage A′ and the gas from stage A′ (stream #5) is sent to stage A. The idea of this configuration is to capture in stage A the carbon that is not separated in stage A′ due to the equilibrium of the carbonation reaction and due to the CO_2 slip during the breakthrough period. From the simulations it was found that it is convenient to cool stream #5 down before feeding it to stage A, since it exits stage A′ at a very high temperature (around 850 °C) with low

carbon content, and therefore the carbonation reaction would not be favored under these conditions in stage A. In absence of this intermediate cooling, stage A would behave more as a bed preheating stage rather than a CO_2 capture stage, which will not provide any significant benefit to the process. For this configuration the operating conditions found as optimum from the sensitivity analysis were used.

In Fig. 12 the axial temperature, solid conversion, gas molar fraction and steam partial pressure profiles inside the reactor in stage A at different moments in time are shown, using an intercooling temperature of 700 °C. It can be seen that in this stage the CaO is converted slowly due to the fact that there is low carbon content in the gases coming from stage A′. A heat plateau at $T_{max,A}$ is also formed during stage A, but at a lower temperature due to the lower amount of CO_2 reacting at the reaction front. In this step hydration is not occurring since the steam partial pressure is always below the equilibrium partial pressure as can be seen in Fig. 12f. The final configuration of stage A is the initial configuration of stage A′, where the fresh charge coming from the adiabatic pre-reformer is fed. In Fig. 13 the axial temperature, solid conversion, gas molar fraction and steam partial pressure profiles inside the bed at different moments in time of stage A′ are shown. It can be seen that the behavior of this step is similar to stage A explained previously. At the entrance of the bed, the CaO has been carbonated to a higher extent compared to the reference case, due to the carbonation of the sorbent in stage A, and the gas fed reacts according to SMR and WGS reactions until the equilibrium of both reactions is reached, which makes the temperature decrease to a value of T_{ad}. The same behavior is obtained for the steam partial pressure and also in this case it is expected that no hydration will occur at the bed inlet, where the H_2O partial pressure is higher than the hydration equilibrium pressure, because the sorbent was already completely carbonated. In Fig. 14 the temperature, gas composition and CCE_{SER} of the outlet stream of stages A and A′ is plotted. As it can be seen in this figure, the CCE_{SER} in stage A is quite stable at around 88% while in stage A' it shows the same behavior of stage A described for the base case. With this two-stage SER step the problem of the carbon loss during the high temperature heat plateau and the breakthrough period is avoided because the slipping carbon is largely captured in the following A stage.

Finally, as a matter of comparison between the balances of the full Ca-Cu process for the reference case shown in Fig. 2 (Case 1), the case using the best operating conditions found from the sensitivity analysis (Case 2) and for the proposed scheme using a two-stage SER process (Case 3), the simulation of the whole process in Fig. 11 was carried out. Also in this case the operating conditions of stages B and C were taken equal to the ones of the reference case. Table 4 shows the carbon mass balances for the three cases. As can be seen, the carbon exiting from stage A with the H_2-rich gas, which will end up as CO_2 emitted to the atmosphere when being burnt in the gas turbine, an improvement of almost 45% can be seen already using optimized operating parameters (Case 2), resulting in an increase of the CCE of the SER stage from 61.4% to 78.4%. The two-stage SER stage in the Ca-Cu process allows reducing the emissions of carbon compounds in the H_2-rich gas per unit of carbon fed to stage A by almost 70% in comparison with Case 1 and by 41% compared with Case 2, further improving the CCE_{SER} to 87.2%. This result confirms the higher CCE reported for this scheme, which results in a global CCE_{tot} of 88% for the whole Ca-Cu process.

The CCE of 88% obtained for the Ca-Cu process scheme depicted in Fig. 11 is similar to the CCE reported in literature for commercial pre-combustion CO_2 capture systems in NGCC based on chemical absorption with amines (i.e. MDEA), which may range between 90 and 92% [23,42]. The autothermal operation of the different

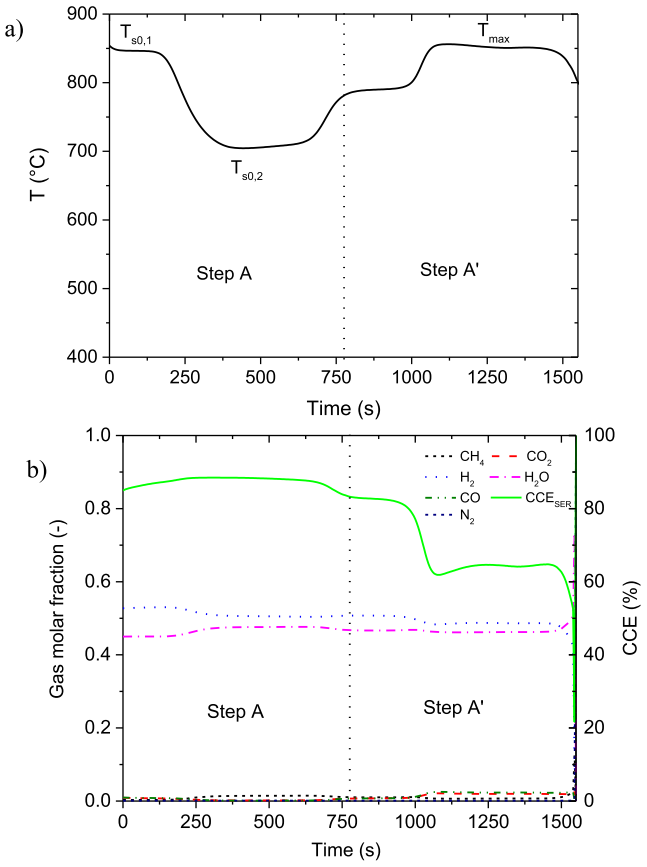

Fig. 14. Temperature (a), composition and carbon capture efficiency (b) of the outlet gas stream of stage A and A′.

Table 4
Mass balances of the complete process for the reference case (Case 1, Fig. 2, Table 3), the case with the best operating conditions found from the sensitivity analysis (Case 2, Fig. 2) and the case with two steps in the SER stage shown in Fig. 11 (Case 3).

	Case 1	Case 2	Case 3
kmol/s of C entering stage A or A′	0.604	0.462	0.462
kmol/s of C entering stage C	0.237	0.254	0.261
kmol/s of C lost from stage A*	0.236	0.100	0.059
kmol/s of C lost from stages B-B′*	0.033	0.031	0.028
kmol/s of C captured in stage C*	0.572	0.585	0.636
CCE_{SER},%	60.9	78.3	87.2
CCE_{tot}, %	68.0	81.7	88.0

* These flow rates are averaged on the cycle time.

reaction stages in the Ca-Cu process allows for a reactor design without high temperature heat transfer surfaces, which are needed in well-established technologies for syngas production based on fired tubular reforming processes. Moreover, the process intensification linked to the Ca-Cu process, where reforming, water gas shift and CO_2 separation stages are integrated in just one stage, as well as the avoidance of dealing with liquid solvents that may lead to operational problems like amine degradation or aerosol formation, represent potential advantages of the Ca-Cu technology. Therefore, even if the CCE reached for this technology when integrated into a NGCC power plant is similar to that reported for commercial technologies, the aforementioned advantages makes the Ca-Cu process a promising second generation capture technology.

4. Conclusions

In this work the performance of the Ca-Cu process using a 1-D pseudo-homogeneous model has been studied. Based on a refer-

ence set of operating conditions where a carbon capture efficiency in the SER stage of 61% and a global CCE lower than 70% was obtained, a sensitivity analysis was carried out in order to assess the influence of different operating parameters of the SER stage on the performance of the process (viz. the total pressure, the inlet gas temperature and the initial bed temperature and the S/C ratio). From this analysis a maximum CCE_{SER} of around 78% was obtained, with process parameters corresponding to a S/C ratio of 5, an initial bed temperature of 700 °C, an inlet gas temperature of 575 °C and 25 bar. A complete cycle with these conditions in stage A was carried out and an overall CCE of 82% was found.

Furthermore, an ideal case was studied assuming the use of an ideal reforming catalyst inactive under 700 °C, in order to have all the reactions occurring at the same reaction front within the solid bed. A CCE of 86% was obtained for this idealized case in the SER stage, which demonstrated that the low CO_2 capture efficiency is largely due to the advancement of the steam methane reforming reaction before the carbonation reaction front.

Finally, two alternative process schemes were proposed in order to increase the CCE: a scheme with a recycle of the H_2-rich stream of stage A and a configuration where the SER stage was split into two stages with an intermediate gas cooling stage. The first configuration did not increase the CCE, mainly due to the reduction of the carbonation reaction kinetics, caused by the lower CO_2 partial pressure associated with the dilution with the recycled H_2. On the other hand, with the second configuration the CCE was increased significantly because the carbon lost from the first SER stage A' was captured in the second stage A. For this new alternative configuration a CCE of 87% was obtained for the SER stage and the overall CCE of the Ca-Cu process was increased to 88%.

Acknowledgements

The presented work is funded within the ASCENT project as part of the European Union's Seventh Framework Programme (FP7/2007-2013) under grant agreement n° 608512. Note: "The present publication reflects only the authors' views and the European Union is not liable for any use that may be made of the information contained therein".

References

[1] IEA, Technology Roadmap – Hydrogen and Fuel Cell, 2015. doi:10.1007/SpringerReference_7300.
[2] J.C. Meerman, E.S. Hamborg, T. van Keulen, A. Ramírez, W.C. Turkenburg, A.P.C. Faaij, Techno-economic assessment of CO_2 capture at steam methane reforming facilities using commercially available technology, Int. J. Greenh. Gas Control. 9 (2012) 160–171, http://dx.doi.org/10.1016/j.ijggc.2012.02.018.
[3] B. Metz, O. Davidson, H. de Coninck, M. Loos, L. Meyer, IPCC special report on carbon dioxide capture and storage, 2005. http://www.google.com/patents/US8119091.
[4] J. Adanez, A. Abad, F. Garcia-Labiano, P. Gayan, L.F. de Diego, Progress in chemical-looping combustion and reforming technologies, Prog. Energy Combust. Sci. 38 (2012) 215–282, http://dx.doi.org/10.1016/j.pecs.2011.09.001.
[5] V. Spallina, B. Marinello, F. Gallucci, M.C. Romano, M. Van Sint Annaland, Chemical looping reforming in packed-bed reactors: modelling, experimental validation and large-scale reactor design, Fuel Process. Technol. 156 (2017) 156–170, http://dx.doi.org/10.1016/j.fuproc.2016.10.014.
[6] F. Gallucci, E. Fernandez, P. Corengia, M. van Sint Annaland, Recent advances on membranes and membrane reactors for hydrogen production, Chem. Eng. Sci. 92 (2013) 40–66, http://dx.doi.org/10.1016/j.ces.2013.01.008.
[7] J.A. Medrano, V. Spallina, M. Van Sint Annaland, F. Gallucci, Thermodynamic analysis of a membrane-assisted chemical looping reforming reactor concept for combined H_2 production and CO_2 capture, Int. J. Hydrogen Energy 39 (2014) 4725–4738, http://dx.doi.org/10.1016/j.ijhydene.2013.11.126.
[8] Z. Chen, F. Po, J.R. Grace, C. Jim Lim, S. Elnashaie, A. Mahecha-Botero, et al., Sorbent-enhanced/membrane-assisted steam-methane reforming, Chem. Eng. Sci. 63 (2008) 170–182, http://dx.doi.org/10.1016/j.ces.2007.09.031.
[9] V. Spallina, D. Pandolfo, A. Battistella, M.C. Romano, M. Van Sint Annaland, F. Gallucci, Techno-economic assessment of membrane assisted fluidized bed reactors for pure H_2 production with CO_2 capture, Energy Convers. Manage. 120 (2016) 257–273, http://dx.doi.org/10.1016/j.enconman.2016.04.073.
[10] D.P. Harrison, Sorption-enhanced hydrogen production: a review, Indus. Eng. Chem. Res. 47 (2008) 6486–6501, http://dx.doi.org/10.1021/ie800298z.
[11] J.R. Hufton, S. Mayorga, S. Sircar, Sorption-enhanced reaction process for hydrogen production, AIChE J. 45 (1999) 248–256, http://dx.doi.org/10.1002/aic.690450205.
[12] Z. Chen, J.R. Grace, C.J. Lim, CO_2 capture and hydrogen production in an integrated fluidized bed reformer-regenerator system, Indus. Eng. Chem. Res. 50 (2011) 4716–4721, http://dx.doi.org/10.1021/ie101360x.
[13] E. Ochoa-Fernandez, G. Haugen, T. Zhao, M. Rønning, I. Aartun, B. Børresen, et al., Process design simulation of H2 production by sorption enhanced steam methane reforming: evaluation of potential CO_2 acceptors, Green Chem. 9 (2007) 654–662, http://dx.doi.org/10.1039/b614270b.
[14] I. Martinez, M.C. Romano, P. Chiesa, G. Grasa, R. Murillo, Hydrogen production through sorption enhanced steam reforming of natural gas: thermodynamic plant assessment, Int. J. Hydrogen Energy 38 (2013) 15180–15199, http://dx.doi.org/10.1016/j.ijhydene.2013.09.062.
[15] H. Boshu, L. Mingyang, W. Xin, Z. Ling, W. Lili, X. Jiwei, et al., Chemical kinetics-based analysis for utilities of ZEC power generation system, Int. J. Hydrogen Energy 33 (2008) 4673–4680, http://dx.doi.org/10.1016/j.ijhydene.2008.06.042.
[16] J. Meyer, J. Mastin, T.K. Bjørnebøle, T. Ryberg, N. Eldrup, Techno-economical study of the zero emission gas power concept, Energy Proc. 4 (2011) 1949–1956, http://dx.doi.org/10.1016/j.egypro.2011.02.075.
[17] R. Kumar, R.K. Lyon, J.A. Cole, Unmixed reforming: a novel autothermal cyclic steam reforming process, Adv. Hydrog. Energy 53 (2000) 31–46, http://dx.doi.org/10.1017/CBO9781107415324.004.
[18] J.C. Abanades, R. Murillo, J.R. Fernandez, G. Grasa, I. Martínez, New CO_2 capture process for hydrogen production combining Ca and Cu chemical loops, Environ. Sci. Technol. 44 (2010) 6901–6904.
[19] I. Martínez, M.C. Romano, J.R. Fernández, P. Chiesa, R. Murillo, J.C. Abanades, Process design of a hydrogen production plant from natural gas with CO_2 capture based on a novel Ca/Cu chemical loop, Appl. Energy 114 (2014) 192–208, http://dx.doi.org/10.1016/j.apenergy.2013.09.026.
[20] J.R. Fernandez, J.C. Abanades, R. Murillo, Modeling of sorption enhanced steam methane reforming in an adiabatic fixed bed reactor, Chem. Eng. Sci. 84 (2012) 1–11, http://dx.doi.org/10.1016/j.ces.2012.07.039.
[21] I. Martínez, R. Murillo, G. Grasa, J.R. Fernandez, J.C. Abanades, Integrated combined cycle from naturale gas with CO_2 capture using a Ca-Cu chemical loop, AIChE J. 59 (2013) 2780–2794, http://dx.doi.org/10.1002/aic.
[22] M. Martini, A. van den Berg, F. Gallucci, M. van Sint Annaland, Investigation of the process operability windows for Ca-Cu looping for hydrogen production with CO_2 capture, Chem. Eng. J. 303 (2016) 73–88, http://dx.doi.org/10.1016/j.cej.2016.05.135.
[23] M.C. Romano, P. Chiesa, G. Lozza, Pre-combustion CO_2 capture from natural gas power plants, with ATR and MDEA processes, Int. J. Greenh. Gas Control. 4 (2010) 785–797, http://dx.doi.org/10.1016/j.ijggc.2010.04.015.
[24] M. Kanniche, R. Gros-Bonnivard, P. Jaud, J. Valle-Marcos, J.M. Amann, C. Bouallou, Pre-combustion, post-combustion and oxy-combustion in thermal power plant for CO_2 capture, Appl. Therm. Eng. 30 (2010) 53–62, http://dx.doi.org/10.1016/j.applthermaleng.2009.05.005.
[25] J.R. Fernández, J.C. Abanades, R. Murillo, G. Grasa, Conceptual design of a hydrogen production process from natural gas with CO_2 capture using a Ca–Cu chemical loop, Int. J. Greenh. Gas Control. 6 (2012) 126–141, http://dx.doi.org/10.1016/j.ijggc.2011.11.014.
[26] J.R. Fernandez, J.C. Abanades, R. Murillo, Modeling of Cu oxidation in an adiabatic fixed-bed reactor with N2 recycling in a Ca/Cu chemical loop, Chem. Eng. J. 232 (2013) 442–452, http://dx.doi.org/10.1016/j.cej.2013.07.115.
[27] G.P. Curran, C.E. Fink, E. Gorin, CO2 acceptor gasification process, in: Fuel Gassification, 1967, pp. 141–165.
[28] M.C. Fuerstenau, C.M. Shen, B.R. Palmer, Liquidus temperatures in the CaCO3-Ca(OH)2-CaO and CaCO3-CaSO4-CaS ternary systems. 1, Indus. Eng. Chem. Process Des. Dev. 20 (1981) 441–443, http://dx.doi.org/10.1021/i200014a006.
[29] T. Numaguchi, K. Kikuchi, Intrinsic kinetics and design simulation in a complex reaction network: steam-methane reforming, Chem. Eng. Sci. 43 (1988) 2295–2301.
[30] Z.S. Li, N.S. Cai, Modeling of multiple cycles for sorption-enhanced steam methane reforming and sorbent regeneration in fixed bed reactor, Energy Fuels 21 (2007) 2909–2918.
[31] I. Martínez, G. Grasa, R. Murillo, B. Arias, J.C. Abanades, Kinetics of calcination of partially carbonated particles in a Ca-looping system for CO_2 capture, Energy Fuels 26 (2012) 1432–1440.
[32] H.P. Hamers, F. Gallucci, P.D. Cobden, E. Kimball, M. van Sint, Annaland, CLC in packed beds using syngas and CuO/Al_2O_3: model description and experimental validation, Appl. Energy 119 (2014) 163–172, http://dx.doi.org/10.1016/j.apenergy.2013.12.053.
[33] J.A. Medrano, H.P. Hamers, G. Williams, M. van Sint Annaland, F. Gallucci, NiO/$CaAl_2O_4$ as active oxygen carrier for low temperature chemical looping applications, Appl. Energy 158 (2015) 86–96, http://dx.doi.org/10.1016/j.apenergy.2015.08.078.
[34] J.R. Fernandez, J.C. Abanades, G. Grasa, Modeling of sorption enhanced steam methane reforming-Part II: simulation within a novel Ca/Cu chemical loop process for hydrogen production, Chem. Eng. Sci. 84 (2012) 12–20, http://dx.doi.org/10.1016/j.ces.2012.07.050.
[35] Z. Li, N. Cai, Y. Huang, H. Han, Synthesis, experimental studies, and analysis of a new calcium-based carbon dioxide adsorbent, Energy Fuels 19 (2005) 1447–1452, http://dx.doi.org/10.1021/ef0496799.

[36] V. Manovic, E.J. Anthony, CO_2 carrying behavior of calcium aluminate pellets under high-temperature/high-CO_2 concentration calcination conditions, Indus. Eng. Chem. Res. 49 (2010) 6916–6922, http://dx.doi.org/10.1021/ie901795e.
[37] V. Manovic, E.J. Anthony, Long-term behavior of cao-based pellets supported by calcium aluminate cements in a long series of CO_2 capture cycles, Indus. Eng. Chem. Res. 48 (2009) 8906–8912, http://dx.doi.org/10.1021/ie9011529.
[38] M. Erans, V. Manovic, E.J. Anthony, Calcium looping sorbents for CO_2 capture, Appl. Energy. 180 (2016) 722–742, http://dx.doi.org/10.1016/j.apenergy.2016.07.074.
[39] A.L. García-Lario, I. Martínez, R. Murillo, G. Grasa, J.R. Fernández, J.C. Abanades, Reduction kinetics of a high load Cu-based pellet suitable for Ca/Cu chemical loops, Indus. Eng. Chem. Res. 52 (2013) 1481–1490.
[40] J.R. Rostrup-Nielsen, J. Sehested, J.K. Nørskov, Hydrogen and synthesis gas by steam- and CO_2 reforming, Adv. Catal. 47 (2002) 65–139, http://dx.doi.org/10.1016/S0360-0564(02)47006-X.
[41] Y.A. Criado, M. Alonso, J.C. Abanades, Kinetics of the CaO/Ca(OH) 2 hydration/dehydration reaction for thermochemical energy storage applications, Indus. Eng. Chem. Res. 53 (2014) 12594–12601, http://dx.doi.org/10.1021/ie404246p.
[42] L.O. Nord, R. Anantharaman, O. Bolland, Design and off-design analyses of a pre-combustion CO_2 capture process in a natural gas combined cycle power plant, Int. J. Greenh. Gas Control. 3 (2009) 385–392, http://dx.doi.org/10.1016/j.ijggc.2009.02.001.
[43] S. Ergun, Fluid flow through packed columns, Chem. Eng. Prog. 48 (1952) 89–94.
[44] D. Vortmeyer, R. Berninger, Comments on the paper, Theoretical prediction of effective heat transfer parameters in packed beds by Anthony Dixon and D.L. Cresswell [AIChE J., 25, 663 (1979)], AIChE J. 28 (1982) 508–510.
[45] D.J. Gunn, M.M.A. Misbah, Bayesian estimation of heat transport parameters in fixed beds, Int. J. Heat Mass Transf. 36 (1993) 2209–2221, http://dx.doi.org/10.1016/S0017-9310(05)80152-8.
[46] D.J. Gunn, Transfer of heat or mass to particles in fixed and fluidised beds, Int. J. Heat Mass Transf. 21 (1978) 467–476, http://dx.doi.org/10.1016/0017-9310(78)90080-7.
[47] M.F. Edwards, J.F. Richardson, Gas dispersion in packed beds, Chem. Eng. Sci. 23 (1968) 109–123, http://dx.doi.org/10.1016/0009-2509(68)87056-3.